

## Graphic analysis of the linear and angular momentum of a dynamically balanced 1-dof pantographic linkage

van der Wijk, Volkert

**DOI**

[10.1007/978-3-030-55061-5\\_38](https://doi.org/10.1007/978-3-030-55061-5_38)

**Publication date**

2020

**Document Version**

Accepted author manuscript

**Published in**

New Trends in Mechanisms and Machine Science

**Citation (APA)**

van der Wijk, V. (2020). Graphic analysis of the linear and angular momentum of a dynamically balanced 1-dof pantographic linkage. In D. Pisla (Ed.), *New Trends in Mechanisms and Machine Science: EuCoMeS: European Conference on Mechanism Science* (pp. 331-338). (Mechanisms and Machine Science; Vol. 89). Springer. [https://doi.org/10.1007/978-3-030-55061-5\\_38](https://doi.org/10.1007/978-3-030-55061-5_38)

**Important note**

To cite this publication, please use the final published version (if applicable). Please check the document version above.

**Copyright**

Other than for strictly personal use, it is not permitted to download, forward or distribute the text or part of it, without the consent of the author(s) and/or copyright holder(s), unless the work is under an open content license such as Creative Commons.

**Takedown policy**

Please contact us and provide details if you believe this document breaches copyrights. We will remove access to the work immediately and investigate your claim.

# Graphic Analysis of the Linear and Angular Momentum of a Dynamically Balanced 1-DoF Pantographic Linkage

V. van der Wijk

*Delft University of Technology, The Netherlands*  
*e-mail: v.vanderwijk@tudelft.nl*

**Abstract.** This article presents a graphical analysis method for the verification of the gravity force balance and shaking force and shaking moment balance of a 1-DoF pantographic linkage. First the joint velocities of the linkage are graphically found of which the procedure is well known. To obtain the linear and angular momentum graphically, the mass and inertia of each element are modeled with two equivalent masses about the center of mass of the element, resulting in a mass and inertia equivalent model with solely point masses. The velocities of these point masses are obtained and each velocity vector is multiplied with the respective mass value to obtain vectors that represent the linear momentum. For force balance it is shown that the sum of all linear momentum vectors form a polygon. Subsequently the linear momentum vectors with their moment arms are transferred into an angular momentum diagram which for moment balance shows to sum up to zero.

**Key words:** Graphic Analysis, Linear and Angular Momentum, Gravity Force Balance, Shaking Force and Shaking Moment Balance, Pantograph.

## 1 Introduction

When mechanisms are shaking force and shaking moment balanced, they do not exert any dynamic reaction forces and moments to their base during (high-speed) motions [3, 5]. This reduces base vibrations significantly and when placed on floating platforms such as drones and cable robot end-effectors, balanced mechanisms do not disturb the position, orientation, and motion of the floating platform [2, 7]. For shaking force balance the linear momentum of all moving elements together must be constant (zero) while for shaking moment balance the angular momentum of all moving elements together must be constant (zero). A shaking force balanced mechanism is also gravity force balanced and therefore all methods for shaking force balancing are also applicable for gravity force balancing.

While there are various methods for force balancing of a linkage, using counter-masses [1] or inherently balanced linkage architectures [6], for moment balancing of a linkage the methods are extremely limited [4]. Obtaining moment balance without additional elements is in most cases not possible [9].

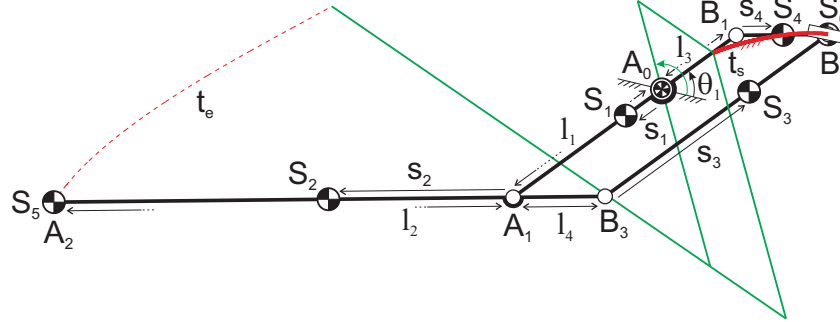


**Fig. 1** 1-DoF dynamically balanced pantographic linkage in two poses with fixed joint  $A_0$  and a slider in  $B_2$  with slider trajectory  $t_s$  in red. The common CoM of all elements is stationary in  $A_0$ .

In order to obtain a better understanding of moment balancing, the goal of this paper is to present a graphical method for the analysis of the linear and angular momentum of a linkage and to apply it to a 1-DoF dynamically balanced pantographic linkage to graphically show that the sums of linear and angular momenta are indeed zero. This will also give insight in the contribution of each linkage element to the total linear and angular momentum, i.e. in their contributions to the dynamic balance.

First the linkage is presented and the joint velocities are found graphically. Then the mass and inertia of each element are modeled with two equivalent masses to obtain a mass and inertia equivalent model with solely point masses. Subsequently the velocities and the linear momenta of the point masses are obtained graphically and are evaluated for force balance. As a final step, an angular momentum diagram is presented for evaluation of the moment balance.

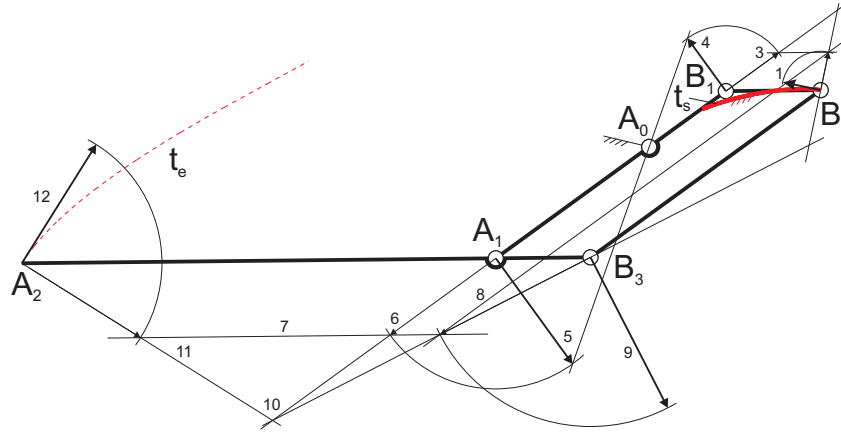
## 2 Graphic Analysis of the Linear and Angular Momentum

Figure 1 shows a pantographic linkage consisting of the 4 links  $B_1A_1$ ,  $B_3A_2$ ,  $B_3B_2$ , and  $B_1B_2$ , which are connected with revolute pairs in  $A_1$ ,  $B_1$ ,  $B_2$ , and  $B_3$ , forming a parallelogram. In  $A_0$  of link  $B_1A_1$  the linkage has a revolute pair with the base, i.e.  $A_0$  is the fixed joint. In joint  $B_2$  there is a slider with fixed slider trajectory  $t_s$  which constrains the linkage to one degree-of-freedom (1-DoF) motion, indicated by angle  $\theta_1$  of the absolute rotation of link  $B_1A_1$ . When in motion, the endpoint  $A_2$  traces the trajectory  $t_e$ . The linkage is shown for two poses, the extended pose at the beginning of the slider trajectory with a relative angle between links  $B_1A_1$  and  $B_3A_2$  of  $35.4^\circ$  and, in green, the retracted pose at the end of the slider trajectory.

The links have lengths  $l_i$  as illustrated in Fig. 1 and each of the 4 links has a mass  $m_i$  and an inertia  $I_i$  about the link center-of-mass (CoM)  $S_i$ , which is at a distance  $s_i$  from a joint as depicted. In addition, in  $A_2$  there is the CoM  $S_5$  of the end-effector

**Table 1** Parameter values for dynamic balance of the pantographic linkage in Fig. 1.

[mm]	[mm]	[g]	[gmm <sup>2</sup> ]
$l_1 = 100$	$s_1 = 24.36$	$m_1 = 118.56$	$I_1 = 312454$
$l_2 = 250$	$s_2 = 100.57$	$m_2 = 302.95$	$I_2 = 2482640$
$l_3 = 50$	$s_3 = 97.05$	$m_3 = 150.19$	$I_3 = 503989$
$l_4 = 50$	$s_4 = 25.48$	$m_4 = 24.22$	$I_4 = 7275$
		$m_5 = 67.16$	$I_5 = 4581$
		$m_6 = 782.63$	$I_6 = n/a$

**Fig. 2** Graphic analysis of the joint velocities with the velocity in  $B_2$  known.

with mass  $m_5$  and inertia  $I_5$ , rigidly mounted on link  $B_3A_2$ , and in  $B_2$  there is the CoM  $S_6$  with mass  $m_6$ , which is the mass of the slider parts and a counter mass together. The inertia of these last parts is not considered since they are solely in translational motion (the slider consists of a pin-in-slot of which the pin is fixed with and included in link  $B_3B_2$  and the piston component that actuates the pin-in-slot motion is moving rectilinearly; the counter mass is a circular disc on the slider pin with negligible friction in between for which it does not rotate). With the values in Table 1 the linkage is completely force balanced and moment balanced, which was verified by a dynamic simulation showing that during motion the common CoM of all elements remains stationary in  $A_0$  and that the sum of the angular momenta of all elements remains zero.

The first step is the graphic analysis of the joint velocities, which is shown in Fig. 2 following the commonly known approach [8]. The velocity in  $B_2$  is known as starting point and has a direction tangent to the slider trajectory  $t_s$ . By rotating it  $90^\circ$ , the intersection (2) with the line through  $A_1B_1$  is found and subsequently intersection (3) and the velocity of  $B_1$  (4) are derived. With the line through  $A_0$  then the velocity of  $A_1$  is obtained (5) which, after  $90^\circ$  rotation (6), determines line (7) which is parallel to line  $A_1A_2$ . The intersection of line (7) with line (8), which is parallel to line  $B_2B_3$ , determines the velocity of  $B_3$  (9). Finally intersection (10) is

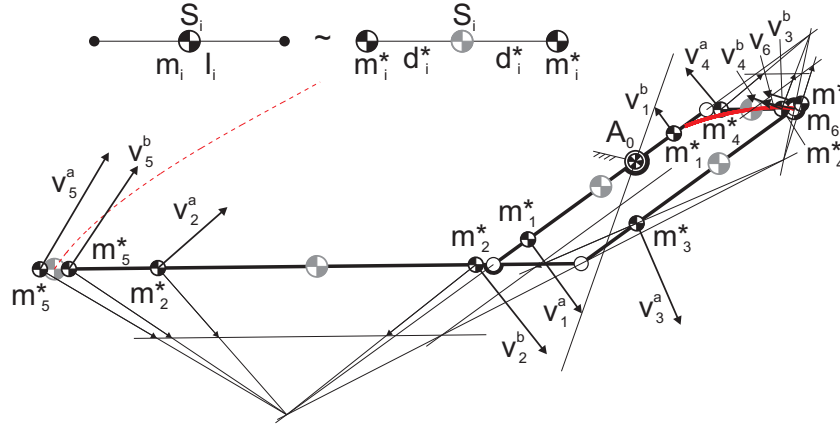


**Fig. 3** Velocity analysis of the point masses of a dynamically equivalent model where the mass and inertia of each element are modeled with two equivalent masses.

obtained with which line (11) to  $A_2$  is determined and the velocity in  $A_2$  is found (12). As expected, the velocity vector in  $A_2$  is indeed tangent to the traced end-effector trajectory  $t_e$ .

To be able to graphically analyze the angular momentum of the linkage, the mass and inertia of each element are modeled with two equivalent masses. This is the simplest possibility for dynamic equivalent modeling of planar motions for which also more than two equivalent masses can be used [10]. Figure 3 shows the dynamically equivalent model where each mass  $m_i$ , except  $m_6$  for which no inertia is involved, has been divided in two equal equivalent masses  $m_i^* = m_i/2$  both located at a distance  $d_i^*$  from the element CoM  $S_i$ , one on each side along the line through the link joints such that  $S_i$  is their common CoM. The distances  $d_i^*$  are determined by the inertia of the element and are derived from  $I_i = 2(m_i^* d_i^{*2})$  as  $d_i^* = \sqrt{I_i/m_i}$  with which the model is both mass and inertia equivalent with solely point masses. It is also possible to divide  $m_i$  in two different equivalent masses with two different lengths  $d_i^*$  or to place the equivalent masses off the line through the link joints which, however, would make the analysis more complicated than needed.

The velocity analysis of the 11 point masses is also shown in Fig. 3. Continuing with the graphical solution of the joint velocities in Fig. 2, with the instantaneous link centers of rotation the velocities of all point masses are readily obtained. This might contrast with the readability of the illustration of Fig. 3, for which the author apologizes.

The linear momentum of each point mass is obtained when each velocity vector in Fig. 3 is multiplied by its mass value. The resulting linear momentum vectors are shown in Fig. 4 which were obtained by multiplying the length of each velocity vector by its respective value  $m_i/100$  with the mass values in Table 1, scaling the vectors to fit within the drawing.

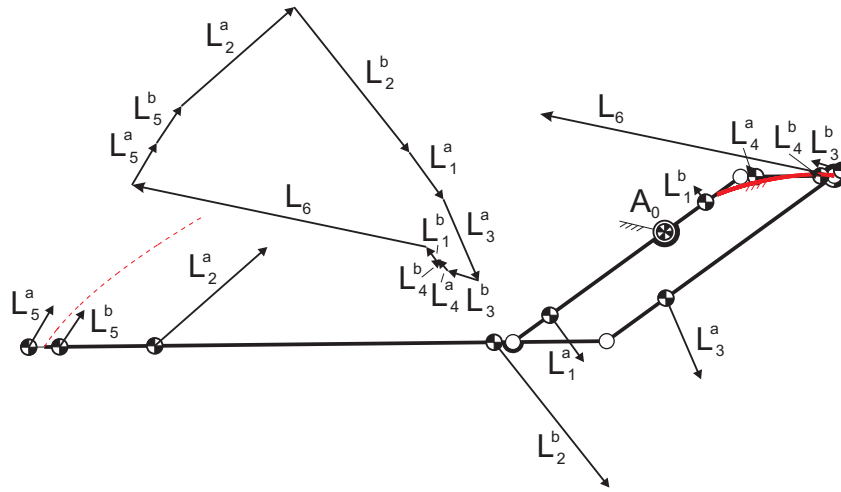


**Fig. 4** Linear momentum vectors obtained by multiplying the velocity vectors with the respective mass values. The sum of the linear momentum vectors forms a polygon for force balance.

The force balance can now be verified by adding all the linear momentum vectors together, which must form a polygon (i.e. a closed chain) since this means that the sum of the linear momenta of the linkage equals zero. The linear momentum polygon is also shown in Fig. 4.

The angular momentum of the linkage consists of the sum of the moments of the linear momentum vectors about the common CoM in  $A_0$ . The moments of the linear momentum vectors are illustrated in Fig. 5 where each linear momentum vector has been shifted along its line of action to the endpoint of its moment arm. The angular momentum diagram in Fig. 6 is obtained from Fig. 5 when all the linear momentum vectors are rotated such that their moment arms are aligned with the same line  $u$ . Then all the linear momentum vectors are oriented vertically, either upwards or downwards.

The angular momentum of each linear momentum vector can be found by the graphical multiplication of lines for which the shown triangle of reference is used with a height of  $L_6$  and a reference width equal to the moment arm of  $L_5^a$ . This results for each linear momentum vector into a diagonal line, which starts at 0 at the location of the vector (i.e. at the end of the moment arm) and crosses the vertical line  $H$  through  $A_0$  - the angular momentum axis - at the value of its angular momentum.

For example, when  $L_2^a$  is placed in the reference triangle at the location of  $L_6$ , which is shown in green, then the diagonal line of  $L_2^a$  is found as the line from the endpoint of  $L_2^a$  to the endpoint of the triangle. Subsequently this diagonal line is placed in the diagram at  $L_2^a$  on line  $u$  and crosses the  $H$ -axis in point  $h$ , which is the value of the angular momentum of  $L_2^a$ .

To sum the resulting angular momentum values, the diagonal lines have been vertically shifted such that each diagonal line starts at the height of the endpoint

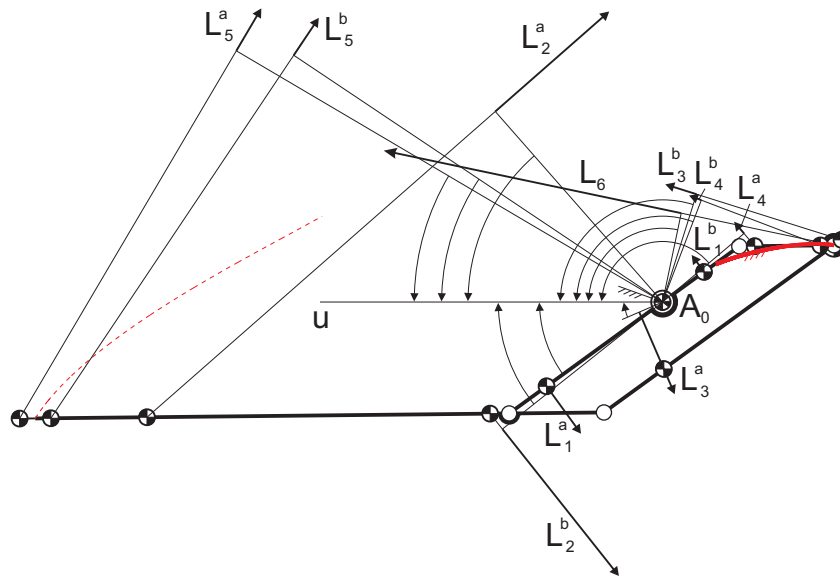


**Fig. 5** Representation of the angular momenta of the linkage with the linear momentum vectors and their respective moment arms about the common CoM in  $A_0$ .

of the previous diagonal line. Of the upward directed linear momentum vectors the summed angular momentum is shown below  $A_0$  and of the downward directed linear momentum vectors the summed angular momentum is shown above  $A_0$ . For the total sum of the angular momenta to be zero, the part above  $A_0$  must be equal to the part below  $A_0$ , which is verified by the circular arc about  $A_0$ .

### 3 Conclusions

In this paper it was shown how the linear momentum and the angular momentum of a linkage can be found graphically. As an example this was applied to verify the shaking force balance and the shaking moment balance of a 1-DoF pantographic linkage. The mass and inertia of each linkage element were modeled with two equivalent masses to obtain a dynamically equivalent model with solely point masses. The velocities of the point masses were derived graphically and the linear momenta of the point masses were found by multiplying the velocity vectors with their respective mass values. For force balance it was shown that the sum of the linear momentum vectors form a linear momentum polygon. The angular momentum was presented in an angular momentum diagram and showed to sum up to zero for moment balance. The presented graphical method may be of help to better understand the characteristics of force balance and, in specific, the characteristics of moment balance for the

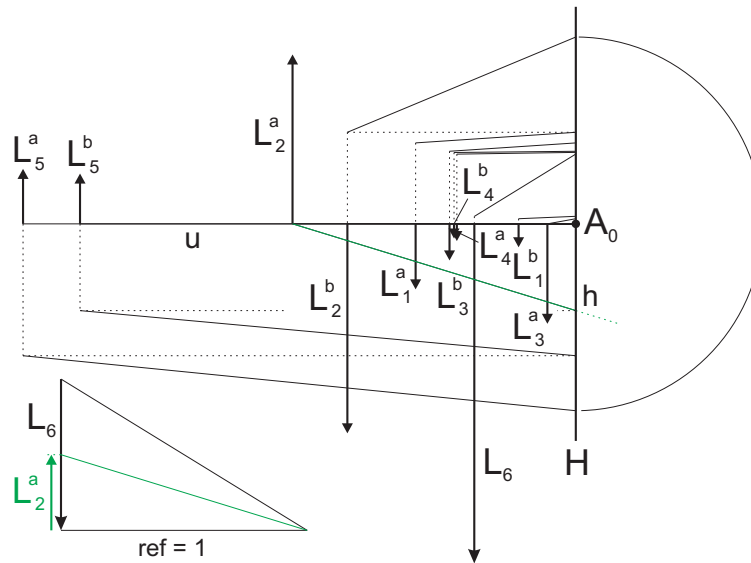


**Fig. 6** Angular momentum diagram obtained by rotating all the linear momentum vectors such that their moment arms are aligned with the same line  $u$ . The angular momentum of each vector is found by the multiplication of lines with the help of a triangle of reference, gaining diagonal lines that intersect with the vertical angular momentum axis  $H$  through  $A_0$  at the angular momentum values. The values of all intersections sum up to zero for moment balance.

development of a synthesis method for moment balanced mechanisms. Extending the method to linkages with multiple degrees of freedom and to spatial linkages is an interesting next step.

**Acknowledgements** This publication was financially supported by the Netherlands Organisation for Scientific Research (NWO, 15146). The author likes to thank Clément Gosselin for the fruitful discussions during the summer and fall of 2018 at Laval University in Quebec City, Canada.

## References

1. Arakelian, V.G., Smith, M.R.: Shaking force and shaking moment balancing of mechanisms: A historical review with new examples. *Mechanical Design* **127**, 334–339 (2005)
2. Foucault, S., Gosselin, C.M.: On the development of a planar 3-dof reactionless parallel mechanism. *Proceedings of DETC 2002, ASME* (2002)
3. Lowen, G.G., Berkof, R.S.: Survey of investigations into the balancing of linkages. *Mechanisms* **3**, 221–231 (1968)
4. Van der Wijk, V.: Shaking-moment balancing of mechanisms with principal vectors and momentum. *J. of Frontiers of Mechanical Engineering* **8**(1), 10–16 (2013)
5. Van der Wijk, V.: Methodology for analysis and synthesis of inherently force and moment-balanced mechanisms - theory and applications (dissertation). University of Twente



- (<https://doi.org/10.3990/1.9789036536301>) (2014)
6. Van der Wijk, V.: The Grand 4R Four-Bar Based Inherently Balanced Linkage Architecture for synthesis of shaking force balanced and gravity force balanced mechanisms. *Mechanism and Machine Theory* **150** **103815** (2020)
  7. Van der Wijk, V., Krut, S., Pierrot, F., Herder, J.L.: Design and experimental evaluation of a dynamically balanced redundant planar 4-RRR parallel manipulator. *I.J. of Robotics Research* **32**(6), 744–759 (2013)
  8. Wittenbauer, F.: *Graphische Dynamik*. Julius Springer, Berlin (1923)
  9. Wu, Y., Gosselin, C.M.: Design of reactionless 3-DOF and 6-DOF parallel manipulators using parallelepiped mechanisms. *IEEE Transactions on Robotics* **21**(5), 821–833 (2005)
  10. Wu, Y., Gosselin, C.M.: On the dynamic balancing of multi-dof parallel mechanisms with multiple legs. *Mechanical Design* **129**, 234–238 (2007)